ELSEVIER

Biomaterials 23 (2002) 3479–3485

Biomaterials

www.elsevier.com/locate/biomaterials

Pitting, crevice and galvanic corrosion of REX stainless-steel/CoCr orthopedic implant material

L. Reclaru[a,*], R. Lerf[b], P.-Y. Eschler[a], A. Blatter[a], J.-M. Meyer[c]

[a] *P.X. Tech, Bldv des Eplature 46, 2304 La Chaux-de-Fonds, Switzerland*
[b] *PI Precision Implants AG Aarau, Switzerland*
[c] *School of Dentistry, University of Geneva, 19 Rue Barthelemy-Menn, 1205 Geneva, Switzerland*

Received 25 June 2001; accepted 8 February 2002

Abstract

The corrosion behavior of surgical implant CoCr alloy and REX 734 steel has been investigated. The pitting or crevice corrosion potentials have been determined to reach values as high as 500 mV vs. SCE for CoCr and 450 mV vs. SCE for REX 734. The galvanic corrosion behavior of CoCr/REX 734 couples has been evaluated with various electrochemical techniques. The measurement of the corrosion current of the galvanic couple as well as its prediction by applying mixed potential theories on measured potentiodynamic polarization curves revealed low galvanic currents in the range of nanoamperes.

Keywords: Electrochemistry; Pitting; Crevice and galvanic corrosion; Stainless steels; CoCr alloy; Orthopedic prostheses

1. Introduction

Corrosion is an essential aspect in the evaluation of biocompatibility, because it plays a crucial role in the release of metal cations into the body environments and in the degradation of the implant. Metallic cations are generated by the processes of electrochemical corrosion or chemical dissolution, and particles can wear off the implant. Such cations and wear debris, concentrated at the implant-tissue interface, may migrate through the tissue.

The evaluation of the corrosion susceptibility of individual and combined materials of an implant therefore becomes an essential aspect in the design of prosthetic devices, since they may be directly related to the design of the implant, the dissimilarity of the materials employed, the nature of the cement, etc. The pertinent types of corrosion of the materials currently used are crevice and pitting corrosion, galvanic corrosion, corrosion fatigue, fretting corrosion, stress corrosion cracking and intergranular corrosion.

In the present study, the corrosion behavior of orthopaedic implant REX 734 stainless steel (ISO 5832-9) and CoCr alloy (ISO 5832-12), as well as their galvanic coupling has been investigated. This combination can be found in modular hip implants, where a ball head of CoCr is tapered on a cemented REX 734 stem.

The infiltration of tissue fluids between the elements of a prosthetic device brings different types of materials into temporary or permanent contact. In this way, two alloys can form a galvanic cell and generate an electric current as a result of their potential difference.

The American Society for Testing and Materials [1] defines a galvanic couple as a pair of dissimilar conductors, commonly metals, in electrical contact. Galvanic corrosion then is the accelerated corrosion of a metal due to an electrical contact with a more noble or non-metallic conductor in a corrosive electrolyte. These definitions introduce two basic concepts: (i) the dissimilarity of the metals which forms the galvanic couple, and (ii) their degree of nobility. Since nobility is defined as the positive (increasingly oxidizing) displacement of the electrode potential against a reference electrode, the evaluation of the dissimilarity of the two components in a galvanic couple becomes a principal concern.

In general, galvanism is represented by simultaneous cathodic and anodic reactions. The cathodic reactions

*Corresponding author. Tel.: +41-32-924-02-90; fax: +41-32-924-01-41.
E-mail address: lucien.reclaru@groupepx.com (L. Reclaru).

0142-9612/02/$ - see front matter
PII: S0142-9612(02)00055-8

consist in the reduction of the dissolved oxygen in the electrolyte

$$O_2 + 4e^- + 2H_2O \rightarrow 4OH^-, \quad (1)$$

$$O_2 + 4H^+ + 4e^- \rightarrow 2H_2O. \quad (2)$$

They take place quickly, and the ease of the reaction increases with the surface area of the cathode and the oxygen saturation of the electrolyte.

The anodic reaction consists in the dissolution of the metal according to

$$M \rightarrow M^{n+} + ne^-. \quad (3)$$

From Eqs. (1)–(3) it can be seen that the electric current generated by the galvanic cell leads, on the one hand, to a local decrease in oxygen and, on the other hand, to an increase in metal ions in solution. The intensity of the galvanic process depends on a number of factors, such as the electrode potential, the polarization, the anode/cathode surface area ratio, the distance between the electrodes, the surface state of the electrodes, the conductivity and the passage of the galvanic current in the electrolytic milieu, diffusion, stirring, aeration, temperature, pH and the composition of the electrolytic milieu.

In addition to galvanism, localized crevice corrosion has also to be taken into account, as this is another design-dependent deterioration mechanism. Local depletion of dissolved oxygen, and particularly the increase in the concentration of metal ions in solution, causes the formation of metal hydroxides followed by a local reduction in the pH,

$$M^{n+} + nH_2O \rightarrow M(OH)_n + nH^+ \quad (4)$$

and the diffusion of Cl^- ions into this zone

$$M^{n+}Cl_n^- + nH_2O \rightarrow M(OH)_n + nHCl. \quad (5)$$

The reduction of the pH and the increase in the concentration of Cl^- ions are two essential factors in the initiation and propagation of the crevice corrosion phenomenon. The acidity of the milieu will increase with time, causing the passive layer of the alloy to dissolve and thus the process of local corrosion to accelerate [2,3].

It is therefore imperative to study the galvanic cell phenomena in multi-metallic reconstitutions together with the crevice corrosion behavior of each component.

2. Materials and methods

The nominal compositions of the test samples are presented in Table 1.

Table 1
Nominal composition of the CoCr alloy and the REX 734 implant steel

CoCr alloy ISO 5832-12		REX 734 steel ISO 5832-9	
Element	Composition (wt%)	Element	Composition (wt%)
C	0.085	Nb	0.25–0.8
N	0.15	N	0.25–0.5
Cr	27.5	Cr	19.5–22
Mo	6.20	Mo	2–3
Mn	0.70	Mn	2–4.25
Si	0.75	Ni	9–11
Fe	<0.65	Si	Max. 0.75
Ni	<0.85	C	Max. 0.08
Co	Balance	S	Max. 0.01
		P	Max. 0.025
		Cu	Max. 0.25
		Fe	Balance

2.1. Pitting or crevice corrosion test

The resistance against pitting or crevice corrosion of the two alloys REX 734 and CoCr were examined according to the standard ASTM F746-87 (reapproved 1994) [4].

The samples for the REX 734 were cut from an orthopedic prosthesis and the samples for CoCr were taken from a bar of diameter 8 mm. The test samples were machined into the form of cylinders of diameter 5 mm and height 10.8 mm, the dimensions of the PTFE collars being modified by a factor of 5/6.35 with respect to the suggestions in the standard. The cylinder surfaces were metallographically polished with 600-grit paper. The samples were not subjected to any special treatment such as heat treatment, hot or cold working, or passivation treatment.

The collar was machined from polytetrafluoroethylene of medical devices purity. The collar's dimensions were: outer diameter 12 ± 0.05 mm, thickness 2.5 ± 0.02 mm, and inside diameters of, respectively, 5.29 ± 0.05 and 4.7 ± 0.05 mm.

The total exposed surface area A_T of the specimen before placement of the collar was 168.8 mm^2. The crevice area A_C (area on the internal surface of the collar) was 39.3 mm^2. The exposed surface area of the specimen after placement of the collar A_S was 129.5 mm^2.

2.2. Galvanic corrosion test

The galvanic corrosion of coupled REX 734/CoCr was evaluated by the direct measurement of the corrosion current of the couple and by prediction of the galvanic current using mixed potential theories and potentiodynamic polarization curves (ASTM G71-81) [5].

2.2.1. Evaluation by the direct measurement of the corrosion current

Discs of diameter 8 mm were prepared from both materials and metallographically polished with diamond paste (2 μm). The discs were then connected to a central stem in order to establish the electrical contact. With this configuration it was ensured that the anode surface was equal to the cathode surface, i.e. their ratio was unity. The couple was subjected to the following measuring cycle:

- Immersion in the electrolyte—de-aerated with Ar for 24 h—for the recording of the open potential of each electrode.
- Recording of the variation of the galvanic current and the common potential of the couple for 24 h.
- Restart after 5 days ; recording of the variation of the galvanic current in the couple for 4 days.

2.2.2. Prediction of the galvanic current by application of the mixed potential theory

The same form of samples (metallographically polished discs of diameter 8 mm) was used. Tafel slopes were derived from polarization curves traced in the range ± 150 mV SCE with respect to the corrosion potential (E_{corr}). Two series of measurements were scanned for each alloy at a rate of 0.1 mV/s.

2.2.3. Prediction of the galvanic current from polarization curves

After 24 h of immersion in the de-aerated electrolyte, the cathodic and anodic potentiodynamic polarization curves were recorded from -1000 to $+1200$ mV vs. SCE at a scan rate of 0.1 mV/s, using a rotating electrode technique with a rotation speed of 300 rpm. A second series of polarization curves was measured in an electrochemical cell as described in ASTM G5-94 [6], i.e. by the static method with a fixed electrode.

2.3. Test equipment

The current vs. time in the galvanic coupling measurement was controlled by an EG&G PAR model 273A potentiostat, which had been modified according to the supplier's instructions to be used as a zero resistance ammeter. This modification permitted measurements of current variations down to 100 pA. The glassy corrosion cell was used with the working electrodes mounted opposite one to the other in the horizontal position. Each electrode was mounted and sealed in PTFE. A saturated calomel electrode (SCE) as the reference and a platinum counter-electrode were used.

2.4. Test milieu

The electrolyte used in the test was a solution of 9 g/l NaCl in de-ionized water (18 MΩ cm) at temperature 37°C. The pH before and after the test was 5.7. The electrolyte was de-aerated with nitrogen. The oxygen concentration in non-de-aerated medium ranged between 5.2 and 6.4 mg/l, whereas it dropped to about 0.2 mg/l in the de-aerated electrolyte, as measured with the Viscolor Oxygen Kit SA 10 (Machery-Nagel-Düren Germany).

3. Results and discussion

3.1. Pitting and crevice corrosion

Two series of samples were measured. In the first series, the tests were run up to 400 mV vs. SCE for CoCr and up to 500 mV vs. SCE for REX 734. The optical examination of the surface below the collar after the test did not reveal any pits, crevices or surface discoloration.

For the second test series, the initial corrosion potentials after immersion for 1 h were -240 mV SCE for CoCr and -45 mV SCE for REX 734. Table 2 presents the current densities recorded after 15 min at the imposed potentials E_1.

Figs. 1 and 2 show the activation curves as recorded during 20 s at 800 mV ($i = f$ (time)) for each imposed potential E_1.

Figs. 3 and 4 display the evolution of the polarizing current densities during 15 min for the various preselected potentials at and above the critical potential for pitting (or crevice) corrosion.

From the analysis of the results of the second series and the optical examination of the surfaces below the collar, we deduce the pitting or crevice potentials to be 450 mV vs. SCE for the CoCr alloy and, respectively, 500 mV vs. SCE for the REX 734 steel. After the tests at or above the crevice potential, the REX 734 samples showed traces of corrosion below the collar (Fig. 5) and the CoCr samples had undergone a surface discoloration.

4. Evaluation by the direct measurement of the corrosion current of the couple

The evolution of the individual potentials of both materials in open-circuit, as well as the variation of the common potential and the galvanic current of the couple once the samples are short-circuited, was measured. Fig. 6 displays the variation of the open-circuit potentials as well as the evolution of the common potential E_{couple} during the first 24 h after coupling.

Table 2
Polarizing current densities of CoCr and REX 734 as measured after 15 min at the imposed potential E_1

Run	E_1 (preselected potential) for measured polarizing current during 15 min (mV)	Polarizing current after 15 min ($\mu A/cm^2$)	Run	E_1 (preselected potential) for measured polarizing current during 15 min (mV)	Polarizing current after 15 min ($\mu A/cm^2$)
CoCr01	−250	−0.0531	Rex01	−100	−0.0688
CoCr02	−200	−0.0297	Rex02	−50	−0.0070
CoCr03	−150	−0.0190	Rex03	0	0.0045
CoCr04	−100	−0.0147	Rex04	50	0.0149
CoCr05	−50	−0.0125	Rex05	100	0.0234
CoCr06	0	-0.0031	Rex06	150	0.0253
CoCr07	50	0.0016	Rex07	200	0.0353
CoCr08	100	0.0106	Rex08	250	0.0410
CoCr09	150	0.0242	Rex09	300	0.0466
CoCr010	200	0.0402	Rex010	350	0.0402
CoCr011	250	0.0616	Rex011	400	0.0554
CoCr012	300	0.0946	Rex012	450	0.0666
CoCr013	350	0.1672	Rex013	500	0.3879
CoCr014	400	0.2664	Rex014	550	1.4509
CoCr015	450	0.5060	Rex015	600	32.240
CoCr016	500	1.086	Rex016	650	45.000
CoCr017	550	2.293			
CoCr018	600	5.147			

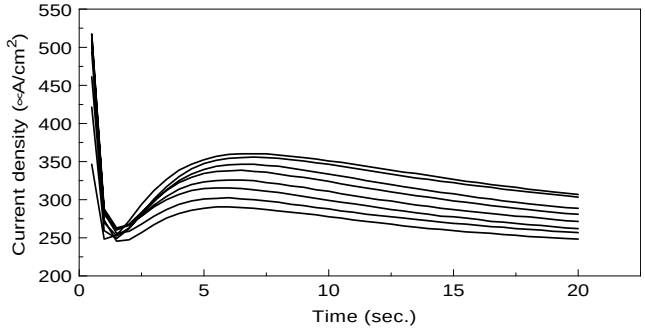

Fig. 1. CoCr alloy; stimulation of localized corrosion at +800 mV vs. SCE.

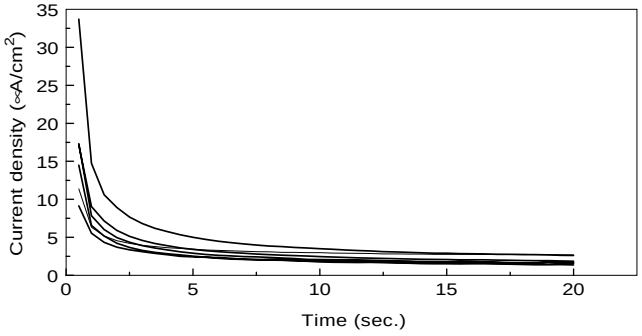

Fig. 2. REX 734 steel; stimulation of localized corrosion at +800 mV vs. SCE.

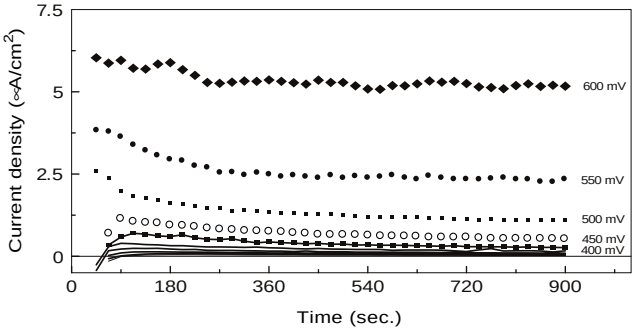

Fig. 3. CoCr alloy; polarizing current densities during 15 min at preselected potentials at and above the critical potential.

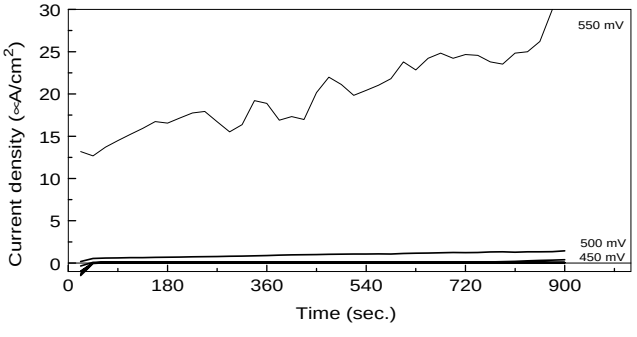

Fig. 4. REX 734 steel; polarizing current densities during 15 min at preselected potentials at and above the critical potential.

Fig. 7 shows the corresponding galvanic current density generated by the couple, $i_{galvanic}$.

The duration of galvanic corrosion tests should be long enough to allow conditions to develop the way they do in service. Galvanic corrosion is frequently time dependent in unpredictable ways. If the desired lifetime of a component is many years, it is often impractical to test for this long a time. In this case, the corrosion

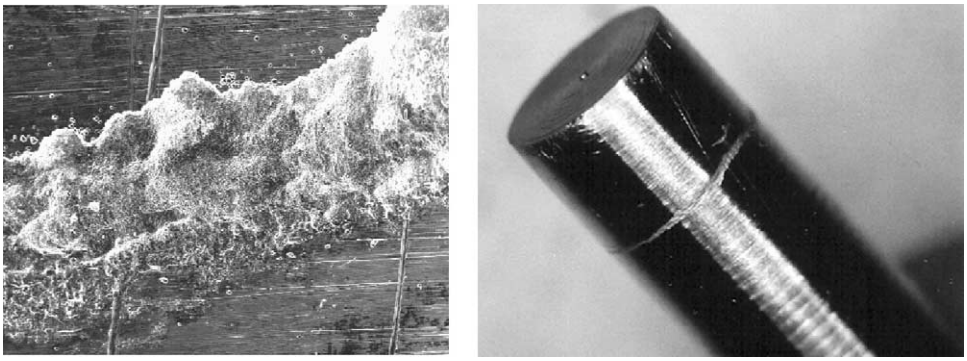

Fig. 5. REX 734 steel; microscopic images of the exposed area under the collar showing crevice corrosion (200X and 7X).

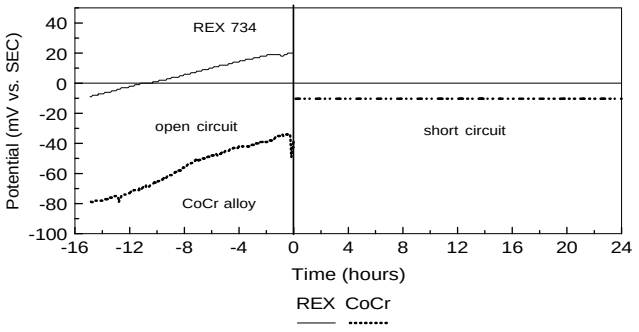

Fig. 6. Open-circuit potential and short-circuit potential vs. time of the REX 734/CoCr couple.

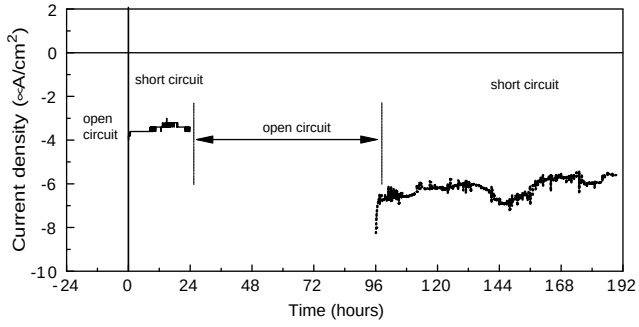

Fig. 7. Galvanic currents vs. time generated by the REX 734/CoCr couple.

process may be followed until a steady state is reached from which extrapolations to long-term service may be justified [7].

It is with this aim that the measurement cycle of our galvanic couple was extended: the sample was kept immersed open-circuit for another 5 days before again being short-circuited to measure $i_{galvanic}$ for further 4 days, as presented in Fig. 7. It can be seen that the recorded current has always stayed negative and constantly low (a few nanoamperes) during this time.

The results of a galvanic measurement are strongly influenced by the ratio of the anode to the cathode surfaces. This ratio was unity in all measurements. The concentration of oxygen dissolved in the electrolyte is another parameter that sensibly affects the galvanic corrosion process, the test milieu being nitrogen de-aerated and the oxygen being controlled throughout the test at a level of approximately 0.2 mg/l.

In summary, the coupled REX 734/CoCr materials exhibit negligible galvanism as evidenced by the low current of the order of nanoamperes generated by the galvanic cell. There is no risk of triggering the phenomenon of crevice corrosion, because the crevice potentials of the alloys are, respectively, 450 and 500 mV SCE as compared to the couple potential E_{couple} of -10 mV SCE. The examination of the surface after the galvanic corrosion tests did indeed not reveal any surface modification, pits, crevices or discoloration.

5. Prediction of galvanic parameters using the mixed potential theory

Galvanic corrosion of alloys can be analyzed by applying the mixed potential theory, as first described by Wagner and Traud [8]. This theory is based on two simple hypotheses: (i) any electrochemical reaction can be divided into two or more oxidation or reduction reactions; and (ii) there can be no net accumulation of electrical charge during an electrochemical reaction. When two different corroding alloys are coupled electrically in the same electrolyte, both alloys get polarized so that each alloy corrodes at a new rate [9]. When applying the mixed potential theory, which consists in a practical method for deriving the sum of cathodic and anodic slopes of the alloys under test, predictive values for E_{couple} and i_{couple} are obtained. Tafel curves are represented here in the linear mode. From polarization curves in the range ± 150 mV vs. E_{corr} we determined the Tafel slopes (a and b) and the corrosion current density (i_{corr}) using the "PAR Calc" routine. The "PAR calc" routine uses all of the data to

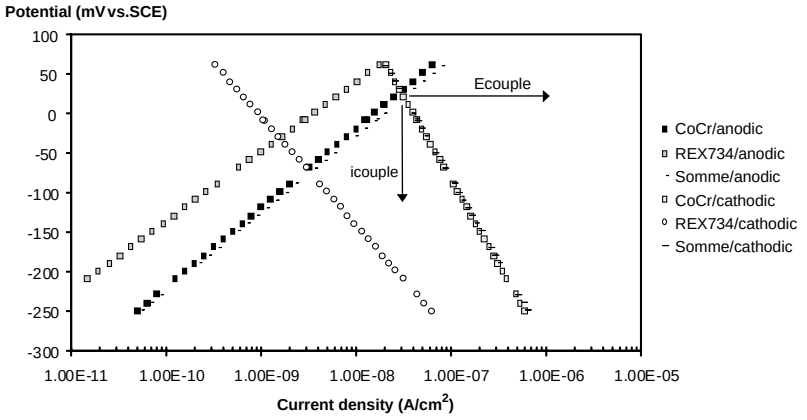

Fig. 8. Application of mixed potential theory to REX 734 steel/CoCr alloy.

perform a non-linear-squares fit of the data to the Stern–Geary equation [10].

In Fig. 8 are displayed the anodic and cathodic slopes, as recorded after 24 h of immersion in de-aerated NaCl electrolyte. The values of i_{couple} and E_{couple} calculated according to the mixed potential theory are also included in the figure. The calculated current is again very low, of the order of nanoamperes, in this approach.

6. Prediction of galvanic parameters from potentiodynamic polarization curves

The data for predicting galvanic parameters from potentiodynamic polarization curves for REX 734 steel and CoCr alloy is shown in Fig. 9 (rotating electrode technique) and Fig. 10 (static method, ASTM electrochemical cell). The rotating electrode technique enables to control the phenomenon of mass transfer according to the theory of Levich [11].

This provides an expression for the Nernst diffusion layer specific to the rotating electrode. In fact, each dissolved species reacting in the electrochemical system has its own Nernst diffusion layer. It is interesting to compare the electrochemical parameters derived from the rotating electrode technique with those from the static system and to verify that there were no significant differences. In our case, the main source for any difference might be related to the control of the oxygen diffusion at the electrode surface.

The fundamental basis of this theory was presented by Wagner and Traud [8], and was also described later by other authors like Hack [12].

The prediction method consists of two steps: (i) plot of the potentiodynamic polarization curves of the two alloys under the same test conditions; (ii) plot of E vs. $\log(i)$ in the same graph. The intersection point of the anodic curve of one alloy with the cathodic curve of the other one returns the predicted coupled potential (E_{couple}) and the galvanic current (i_{couple}).

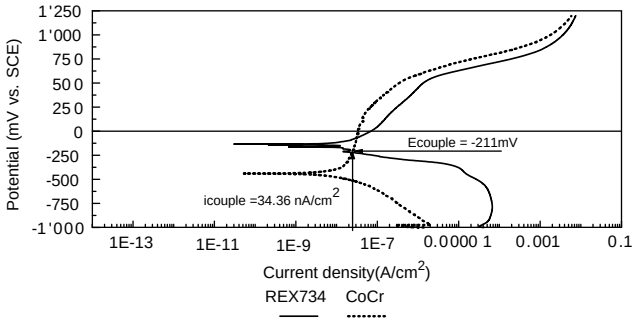

Fig. 9. Prediction of the coupled potential and galvanic current density from potentiodynamic polarization curves for REX 734 steel and CoCr alloy; rotating electrode technique.

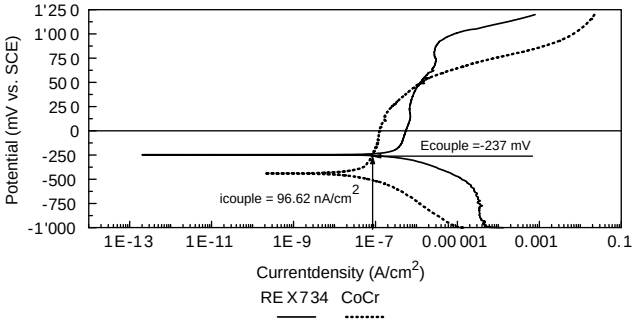

Fig. 10. Prediction of the coupled potential and galvanic current from potentiodynamic polarization curves for REX 734 steel and CoCr alloy; fix electrode technique.

These intersection points are highlighted by arrows in Figs. 9 and 10 showing the values of E_{couple} and i_{couple} as predicted by this method. We notice that the predicted currents are of the same order of magnitude, and they remain low.

The comparison of the values derived from the rotating electron technique (Fig. 9) with those from the fixed electron technique (Fig. 10) reveals indeed some discrepancy concerning the diffusion time of the

Table 3
Summary of electrochemical parameters, galvanic current and coupled potential

Techniques, methods	$E_{couple\ corr}$ (mV SCE)	$i_{couple\ corr}$ (nA/cm^2)
Direct measurement	−10	6.50
Application of the mixed Potential theory	+21	32.64
Polarization curves; fix electrode	−237	96.62
Polarization curves; rotating electrode	−211	24.36

oxygen at the electrode surface; however, we do not consider this difference to be significant.

7. Summary electrochemical aspect of coupled REX 734 steel/CoCr alloy

In Table 3 are summarized the results of the galvanic coupling as obtained by the various measurement techniques. All the different techniques lead consistently to the conclusion that the galvanic currents (whether measured or calculated) are low.

8. Conclusion

The galvanic current of the CoCr/REX 734 couple, whether evaluated by direct measurement or by prediction theory, is very low, of the order of some tens of nanoamperes. When electrically coupled, the CoCr becomes the anode while the REX 734 is the cathode.

In the orthopedic implant device, the surface ratio of the CoCr ball and the REX 734 stem is $8678\,mm^2/6079\,mm^2 = 1.43$. This represents an even favorable situation for the Cocr alloy, as the anodic current densities, and hence the corrosion rate will be further diminished with respect to our test assembly with a surface ratio of 1.

With 500 mV for the CoCr and 450 mV for REX 734, the crevice potential of both materials examined are very high, much higher than the galvanic potential of the coupled material. In consequence, there is no appreciable risk for a crevice corrosion caused or amplified by the galvanic coupling.

References

[1] Standard guide for development and use of galvanic series for predicting galvanic corrosion performance, ASTM G82-83 (reapproved 1993), Wear and Erosion; Metal Corrosion, ASTM vol. 03.02. Philadelphia: ASTM, 1998. p. 341–7.
[2] Sharland SM, Tasker PW. A mathematical model of crevice and pitting corrosion. The physical model. Corros Sci 1988;28:603–21.
[3] Sato N. Towards a more fundamental understanding of corrosion processes. Corrosion 1989;45:354–68.
[4] Standard test method for pitting or crevice corrosion of metallic surgical implant materials, ASTM F746-87 (reapproved 1994), Medical Devices and Service, vol. 13.01, Philadelphia: ASTM, 1998. p. 187–92.
[5] Standard guide for conducting and evaluating galvanic corrosion tests in electrolytes, ASTM G71-81 (reapproved 1992), Wear and Erosion; Metal Corrosion, ASTM vol. 03.02. Philadelphia: ASTM, 1998. p. 262–5.
[6] Standard reference test method for making potentiostatic and potentiodynamique anodic polarization Measurements, ASTM G5-94, Wear and Erosion; Metal Corrosion ASTM vol. 03.02. Philadelphia: ASTM, 1998. p. 54–64.
[7] Hack HP. Galvanic corrosion test methods. NACE International Houston Texax, Syrett B.C., Series Editor, 1993;11–8.
[8] Wagner CV, Traud WZ. Uber die Deutung von Korrosionsvorgangen durch Uberlagerung von elektrochemischen Teilvorgangen und uber die Potentialbildung an Mischeelectroden. Zeitschrift fur Elektrochemie und angewandte physikalische Chemie. Elektrochem 1938;44:391–454.
[9] Baboian R. Electrochemical techniques for predicting galvanic corrosion. In: Baboian R, France Jr. WD, Roew LC, Rynewicz JF, editors. Galvanic and pitting corrosion-field and laboratory studies, ASTM STP 576. Philadelphia: American Society for Testing and Materials, 1976. p. 6–19.
[10] Stern M, Geary AL. Electrochemical polarization. I. A theoretical analysis of the shape of polarization curves. J Electrochem Sci 1957;104:56–63.
[11] Adams RN. §4–3. Stationary electrodes in flowing solution. In: Electrochemistry at solid electrodes. New York: Marcel Dekker, 1969. p. 76–107.
[12] Hack HP. Evaluation of galvanic corrosion. In: Metals handbook, Corrosion, vol. 13. Metals Park, Ohio: ASM International, 1987. p. 234–8.